ELSEVIER

Journal of Nuclear Materials 241–243 (1997) 804–809

journal of nuclear materials

Time resolved observation of the erosion of boron containing protective coatings on wall elements of TEXTOR-94 by means of colorimetry

P. Wienhold [a,*], F. Weschenfelder [a], J. von Seggern [a], B. Emmoth [b], H.G. Esser [a], P. Karduck [c], J. Winter [a]

[a] *Institut für Plasmaphysik, Forschungszentrum Jülich GmbH, Ass. EURATOM-KFA, D-52425 Jülich, Germany*
[b] *Physics Department Frescati, KTH Stockholm, Ass. EURATOM-NFR, S-10405 Stockholm, Sweden*
[c] *Gemeinschaftslabor für Elektronenmikroskopie, RWTH Aachen, D-52070 Aachen, Germany*

Abstract

The paper describes the investigation of the progressive erosion of an a-B:D coated test piece during 22 pulses in the SOL of TEXTOR-94. Time resolved observations by colorimetry reveal that the erosion proceeds in steps: during an intermediate phase the rates do not exceed ≈ -1.5 nm/s. Thereafter they jump to about -6 nm/s. This is due to carbon incorporation and triggered when the concentration approaches $\approx 40\%$. The changing composition may influence the ratio of the BII/CII emission near the surface. The process ends with a carbon rich layer on the remnants of the boron film. Combination of different investigations (AES, NRA, EPMA) results in a preliminary model description.

Keywords: Erosion and particle deposition; Low Z wall material; Chemical erosion; SOL plasma; Analytical model

1. Introduction

Carbon erosion from wall elements (limiter, divertor) is still a major concern in fusion devices [1]. Thin boron containing coatings can protect the surface and prevent the tokamak plasma from oxygen and impurity release for a limited time [2]. Despite erosion due to the hydrogen the coatings are partly reformed by simultaneous deposition of impurities eroded at other locations and transported in the scrape-off layer (SOL) [3]. This can change the composition of the near surface layer of the coating and hence the resistivity against erosion. Its life time can increase remarkably [4]. It depends on the balance of erosion and deposition fluxes which decay radially with distance from the plasma edge. The complex patterns depend on the shape of wall elements. Investigations of large areas are of importance in order to understand the erosion and deposition processes and to develop proper in-situ repair techniques [5]. The paper describes briefly in its first part the colorimetric observation of the progressive erosion of a pure a-B:D protective film on a test piece exposed in the SOL plasma of TEXTOR-94. The technique [6] and part of the results [4] have recently been published. The emphasis is laid on the spectroscopic observations and on the post mortem analysis made by means of AES sputter depth profiling and by ion beam analysis. The combination of the results leads to a model which can describe quantitatively the erosion rates in terms of the particle fluxes and as a function of time and of distance from the plasma edge. The model remains preliminary, however, since considerable boron reflux has to be assumed which could not be proven experimentally.

2. Experimental

Colorimetry measures the color coordinates (R, G, B) of the interference colors of transparent coatings appearing

* Corresponding author. Tel.: +49-2461 613 203; fax: +49-2461 612 660; e-mail: p.wienhold@kfa-juelich.de.

PII S0022-3115(96)00610-1

in illuminating white light by means of a color CCD camera. Their relation to the film thickness is calibrated within the range 30 to 500 nm [6]. Image processing yields contour lines over extended areas. For the erosion experiment, a preboronized (between 95 and 110 nm pure a-B:D on an Al interlayer of $\approx$ 300 nm) graphite tile was brought into the SOL and exposed during 22 discharges (121.3 s). Because its plane surface (60 mm $\times$ 63 mm) was tilted to the toroidal direction ($\delta = 20.8°$) the different surface locations corresponded to different radial distances from the plasma edge ($r_a = 46.0$ cm) and covered the radial range of 47.2–49.5 cm (see Fig. 2). This tile was screwed on a graphite block. The block was shielded by Al-plates (2 mm thick) to avoid carbon sputtering. The surface to be eroded pointed to the ion drift side with about 40 m field line distance to the next neighbored limiter. Most of the plasma pulses (≈ 7 s duration, $n_e = 2.5 \times 10^{13}$ cm^{-3}, $I_p =$ 350 kA, $B_T = 2.25$ T) were auxiliary heated for 2 s by neutral beam co-injection (NBI) of 1.3 MW. This increased the density $n(r_a)$ and the temperature $T(r_a)$ at the last closed flux surface (LCFS) from 2.4 to 6.2×10^{12} cm^{-3} and from 25 to 44 eV, respectively [7]. During the exposures the emitted BII light was observed from side and top by CCD cameras. The ratio BII/CII was determined by a spectrometer viewing the probe from the side 20 mm apart from its right end. Its slit covered the radial range $r \approx 48$–44 cm (cf. Fig. 2). After each pulse the changed color patterns were recorded and thickness profiles scanned with 0.2 mm space resolution in toroidal direction at 10 different poloidal locations. There was little thickness variation in poloidal direction only, thus the data have been averaged resulting in one single profile with a statistical error of $\approx$ 10%. The deposit was analyzed post mortem across the surface in toroidal direction by means of sputter depth profiling with Auger electron spectroscopy (AES), by nuclear reaction analysis (NRA) to measure the amount of boron, and by electron probe micro-analysis (EPMA) to quantify also other incorporated components (Si, Al, C).

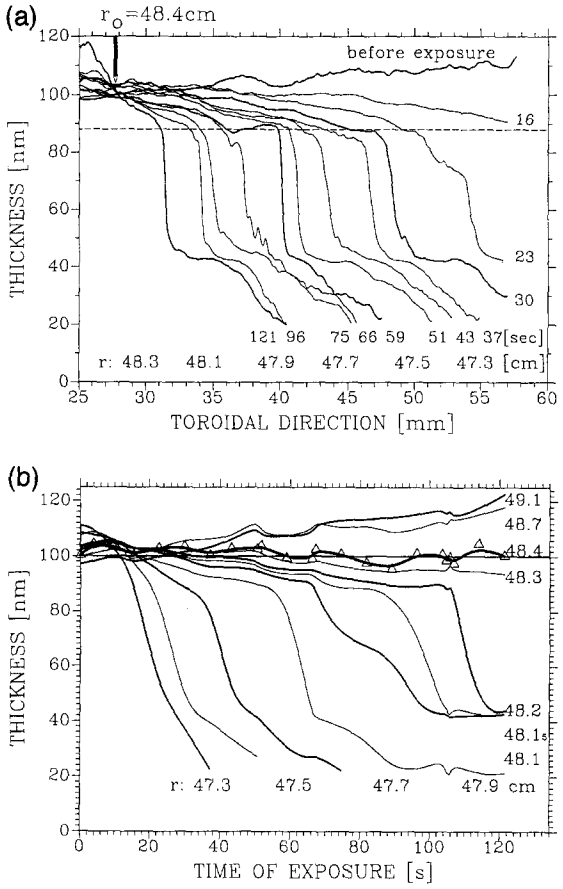

Fig. 1. (a) Thickness profiles in the erosion dominated zone as measured by colorimetry. The total exposure times elapsed are given. Because of the tilted surface different toroidal locations correspond to different distances r from plasma center. At $r_0 =$ 48.4 cm net erosion turns into net deposition. (b) Time evolution of thicknesses as evaluated from (a) at different radial distances. At $r_0 = 48.4$ cm the thickness remains constant throughout the whole exposure time of 121.3 s.

3. Observations

3.1. Colorimetry

Fig. 1a summarizes the evolution of the film thickness in the erosion dominated zone in form of profiles along the toroidal direction of the tile. This direction corresponds — because of the tilting — to increasing radial distances r from the plasma center. Due to the erosion by the D^+-ions in the SOL the initial film thickness of 100–110 nm in this zone is reduced pulse by pulse. A sharp edge is formed with a sudden drop by more than 40 nm. The edge moves radially outward over the tile with decaying speed (characteristic time $\tau_E \approx 37$ s) and creeps against a location corresponding to the radial distance $r_0 = 48.4$ cm ('transition point') where net erosion turns into net deposition. Here, the impurity deposition (mainly carbon) exceeds the erosion by D^+, and the thickness increases gradually with a maximum increment of $\approx$ 25 nm at $r = 49.1$ cm (end of the information range; not shown). This can better be seen from the time evolutions of the thicknesses at selected radii as evaluated from the profiles (Fig. 1b). The curves are splines through the somewhat scattering data. One example (triangles) is given for $r_0 = 48.4$ cm where the thickness remains constant throughout the whole exposure time. The erosion process proceeds in three pronounced steps: (i) the first $\approx$ 20 nm (dashed line in Fig. 1a) are eroded slowly with rates between 0 and about -1.5 nm/s, strongly depending on r. The times (t_m) for this 'inter-

mediate' erosion last from 20 s ($r = 47.4$ cm) up to 110 s ($r = 48.2$ cm); (ii) thereafter the rates jump abruptly to ≈ -6 nm/s almost independent from r and last until further 40–50 nm are eroded ('peak' erosion); (iii) eventually, the rates decrease again and seem to level off. Thicknesses less than ≈ 20 nm are difficult to measure.

3.2. Spectroscopy

As an example Fig. 2 shows the characteristic BII emission light pattern during the NBI phase of one of the discharges. The contour lines correspond to intensity steps of 20% each beginning in the center. The maximum radiation at $r_i = 46.6$ cm appears between the LCFS and the end of the tile. This is due to boron leaving the surface and is consistent with the short ionization length [8] of 0.6 cm under the conditions present at $r = 47.2$ cm. It also means that part of the boron can be redeposited. The BII light intensity measured by the spectrometer decreased during the sequence of discharges and reached an almost stationary level with a characteristic time $\tau \approx 29$ s. This value corresponds to the time τ_E and indicates the shrinking area of the a-B:D layer on the tile itself as the source of the radiating boron. The CII light intensity decreased very slightly and followed the general trend of that of CV measured in the plasma center. It indicates the background flux as the major carbon source in the SOL. Part of the C-ions hitting the surface are reflected and re-ionized, part of them remain deposited and increase the carbon concentration in the surface near layer. The BII/CII ratio approached a stationary value corresponding to about 25% B^+-ions related to carbon [7]. Carbon accumulates in the film and becomes increasingly eroded, but the contribution to the CII light seems to be hidden by the dominant background flux.

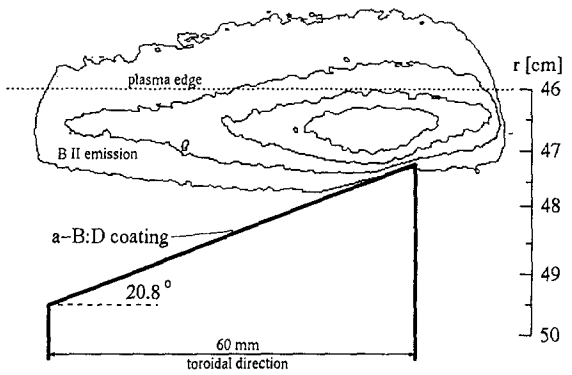

Fig. 2. BII emission light pattern observed above the tilted surface by a CCD camera during the NBI phase of one of the discharges. The contours represent intensity steps of 20% each beginning in the center at $r_i = 46.6$ cm. Left is ion drift side.

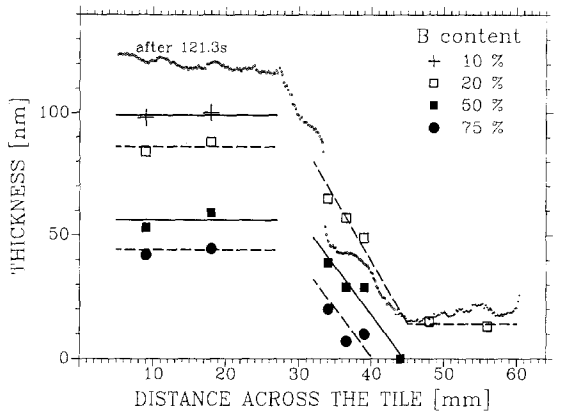

Fig. 3. Concentrations of boron as determined by AES sputter depth profiling at 7 locations across the tile in toroidal direction. The thicknesses are recalculated from the transition to the Al substrate. For comparison the last measured thickness profile (dots) is given.

3.3. Post mortem analysis

Indeed, the AES depth profiling carried out at 7 different locations across the tile revealed that the erosion/deposition process had left a carbon rich layer (a-C/B:D) on top of the remnants of the initial a-B:D film. The results summarized in Fig. 3 show that the B-content (related to C and the other implanted impurities) becomes less than 20% near the surface (crosses and boxes). The thickness scale is recalculated from the depth of the interface to the Al-interlayer. The 50% line (squares) may indicate the transition to the virgin a-B:D. For better comparison a thickness profile (dotted) is given which was measured colorimetrically after the end of the experiment. Except the enrichment of carbon in the upper ≈ 20 nm and the loss of boron in the erosion zone, we observe in the deposition zone (left part of the figure) considerable less boron than measured initially and its replacement mainly by carbon. This is backed by the determination of the boron areal densities by NRA (7.8×10^{17} cm^{-2}) and by EPMA (6.0×10^{17} cm^{-2}) which would represent thicknesses of 78 and 60 nm, respectively ($\rho_{a\text{-}B:D} = 1.0 \times 10^{23}$ B/cm^3 [4]). The rest up to about 120 nm is due to incorporated carbon and silicon ($\approx 10\%$) which was present because of proceeding silane puffing experiments. Moreover, about 150 nm Al of the interlayer was eroded at the very end of the tile (right) where nevertheless a thin deposit still exists which consists of a mixture of Al, C and B. It seems that this layer is very resistant against erosion and may cause the eventual drop in the erosion rate when the thickness falls below about 40 nm. The observations suggest that impurities transported in the SOL can be incorporated into regions (≥ 20 nm) deeper than implantation depth (few nm) of the ions

independent on whether the process leads to net erosion or deposition.

4. Modeling

4.1. A simple equation

The fact that erosion turns into deposition at the fixed radial distance $r_0 = 48.4$ cm suggests a stable ratio between the eroding hydrogen flux $\Gamma_D(r)$ and the impurity (mainly C) deposition flux $\Gamma_c(r)$ in the SOL [9], but with different decay lengths λ_D and λ_C. This leads to the simple equation

$$\mathrm{d}E\,(\text{particles cm}^{-2}\ \text{s}^{-1}) = \left\{\Gamma_C(r_0)\mathrm{e}^{-(r-r_0)/\lambda_C} - Y\Gamma_D(r_0)\mathrm{e}^{-(r-r_0)/\lambda_D}\right\}\sin\delta \quad (1)$$

which should describe the net erosion or deposition $\mathrm{d}E$ in a first approximation. $\delta = 20.8°$ is the tilt angle, Y the sputter yield by D^+-ions. $\Gamma_D(r_0) = 1.7 \times 10^{18}$ cm^{-2} s^{-1} and $\lambda_D = 1.1$ cm are figured out of the n_e, T_e values at the LCFS and by means of their radial decay in the SOL [7] and giving consideration to the ohmic and the NBI heated phases of the plasma pulse. The impurity flux was not measured, but has to be consistent with the observed net erosion/deposition. If we interpret the deposit found on the Al shielding plate at $r = 49.8$ cm (1.36×10^{18} cm^{-2} determined by EPMA) as grown in 121.3 s by a carbon flux with $\lambda_C \approx 2$ cm [3] we find $\Gamma_C(r_0) = 2.26 \times 10^{16}$ cm^{-2} s^{-1}. The flux ratios Γ_C/Γ_D between 0.8% and 2% depend on r, but correspond to earlier observations [10]. Y is the last free parameter in Eq. (1) to fit the data. As the amorphous boron contains some carbon we expect $Y \approx 0.01$ [11,12]. The best fit yields $Y = 0.0135$ for the measured intermediate rates (Fig. 4). The circles are calculated by an extended equation (next chapter). As shown earlier [4] Eq. (1) can describe also the much higher 'peak' erosion rates if the sputter yield Y is set to an accordingly higher value. The reason for the sudden increase remained unclear, however. As will be pointed out the jump of the rate is likely due to the further admixing of carbon up to higher concentrations c. If e.g. $c(t)$ exceeds about 40% in the a-C/B:H film the sputter yield Y increases by factors 3–5 for low energy H_2^+ [13] and H_2^+ and D_2^+ [14] ions. The time t_m to achieve the changeover from intermediate to peak erosion should therefore indicate that the concentration $c(t)$ in the surface near layer has reached such a value. This, however, is not correctly described by Eq. (1) and the fluxes assumed here which yield times less than ≈ 20 s at e.g. $r = 48.2$ cm while $t_m \approx 106$ s is observed.

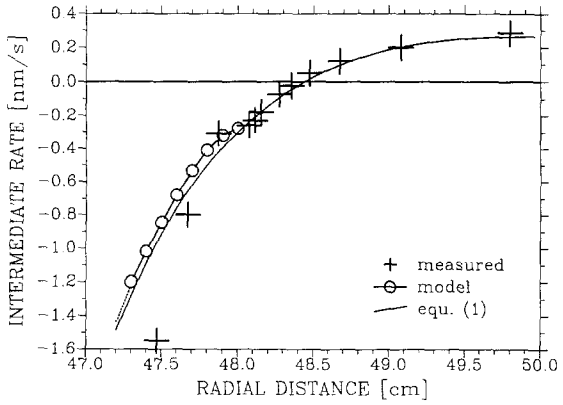

Fig. 4. Intermediate rates and deposition rates as measured (crosses) across the tile depending on radial distance and comparison (thick line) to the model Eq. (1) with $Y = 0.0135$. Calculations made with the extended model (circles) include boron redeposition in the erosion zone.

4.2. Extended model equation

In order to decelerate the evolution of the carbon concentration $c(t)$ the direct redeposition [15] of part of the eroded boron has to be assumed. This is not unlikely because of the short ionization length $\lambda_B \approx 0.6$ cm adjacent the end of tile during the NBI phase. The B^+-flux may also radially be distributed with a similar decay length in a first approximation. It decays with the characteristic time $\tau \approx 29$ s, most likely due to the shrinking source area ($\tau_E \approx 37$ s). This leads to a factorization in time t and space r of the B^+ redeposition flux which has to be added to the balance Eq. (1):

$$\Gamma_B(r, t) = \Gamma_B^+(r, 0)\mathrm{e}^{-t/\tau}\sin\delta, \quad (2)$$

$$\Gamma_B^+(r, 0) = 1/\lambda_B\Gamma_B(0)\mathrm{e}^{-(r-r_i)/\lambda_B}, \quad (3)$$

$$\Gamma_B(0) = \tfrac{1}{2}\int Y\Gamma_D(r)b(0)\,\mathrm{d}r. \quad (4)$$

$\Gamma_B(0)$ is integrated within the radial extension $r_1 = 47.2$ cm, $r_2 = 49.5$ cm of the tile and may represent the initially ($t = 0$) eroded amount of boron. 50% of it may flow to the electron drift direction. Since the boron concentration $b(0) \equiv 1$ the prefactor $1/\lambda_B\Gamma_B(0)$ in Eq. (3) becomes 5.5×10^{16} cm^{-2} s^{-1}.

The erosion of C and B are assumed to be proportional to their actual concentrations $c(t)$ and $b(t)$. Conservation of the initial number of particles $N_B(0)$ (cm^{-2}) is assumed in the considered layer volume which is represented by the increment $\Delta = N_B(0)/\rho_{a\text{-}B:D}$. This means that the particle loss $\mathrm{d}E(t)$ at the surface is currently be replaced by a flux $F_B = -\mathrm{d}E$ of 'fresh' boron through the interface. Discretisation in time steps $\mathrm{d}t$ finally yields the time evolution

of the carbon concentration $c(t)$ and the total erosion $E(t)$ at a location r:

$$c(r, t) = N_C(t)/N_B(0), \tag{5}$$

$$N_C(t + dt) = N_C(t) + [\Gamma_C(r) - Y\Gamma_D(r)c(r, t)]\,dt \quad \text{with } N_C(0) = 0, \tag{6}$$

$$E(r, t) = \sum dE(r, t)\,dt, \tag{7}$$

$$dE(r, t) = \Gamma_C(r) - Y\Gamma_D(r) + \Gamma_B(r, t). \tag{8}$$

Redeposition of the eroded carbon (mainly in the form of CD_x radicals [16]) is not considered because of ionization lengths > 12 mm [8].

4.3. Fitting procedure

Since both carbon and boron deposition fluxes are not measured, the fitting procedure shall proof only the suggestion that boron redeposition can decelerate the evolution $c(r, t)$ in agreement with the observed intermediate times $t_m(r)$ and the erosion rates. Whether the redeposition of boron is fully described by Eqs. (2)–(4) is rather uncertain. But, as a consequence of the additional flux Γ_B in Eq. (8) the one for carbon should be less than assumed in Eq. (1) in order to fit the net rates still correctly. Factors $f^B(r)$ and $f^C(r)$ have therefore been applied to the fluxes Γ_B and Γ_C and varied until the fit condition was satisfied: $c(r, t)$ should approach 40% within the measured intermediate times $t_m(r)$ while $E(r, t) = -20$ nm. Here, the eroded thickness E is calculated with $\rho_{a\text{-}C/B:D} = 6.5 \times 10^{22}$ cm^{-3} [6]. The third fitting parameter Δ is the thickness of the involved layer. Because of the boundary conditions for the parameters and the great number of data there was little freedom of choice. As an example Fig. 5 shows that only $\Delta \approx 21$ nm fits the time $t_m \approx 28$ s valid for $r = 47.6$ cm ($f_B = 2.15$, $f_C = 0.61$). Such values for Δ were found also for the other radii in the erosion dominated zone. It strongly limits the fitting scenarios and determines the relations $f(r)$. As expected, the factor f^C for $\Gamma_C(r)$ is below unity and ranges between 0.8 and 0.5 for $r = 47.3$ and 48.1 cm, respectively. Other values cause disagreement with the measured rates and times. f^B increases from ≈ 1 to ≈ 9 in this range and means that an enhanced boron reflux has to be assumed compared to Eqs. (2)–(4) to fit the data. If $\Gamma_B(r, t)$ is split into a term Γ_B^+ according to Eq. (3) the additive term $\Gamma_B^n(r, t) \approx 1.6 \times 10^{16}(r - 47.4)e^{-t/\tau}$ becomes proportional to r. Note, that both of the terms are almost negligible after about 60 s. However, the mechanism responsible for the enhanced B-reflux is not clear yet. Until simulations by means of the ERO-TEXTOR code [17] are done, we only can speculate that the contribution Γ_B^n might probably be due to boron which remains neutral after the erosion.

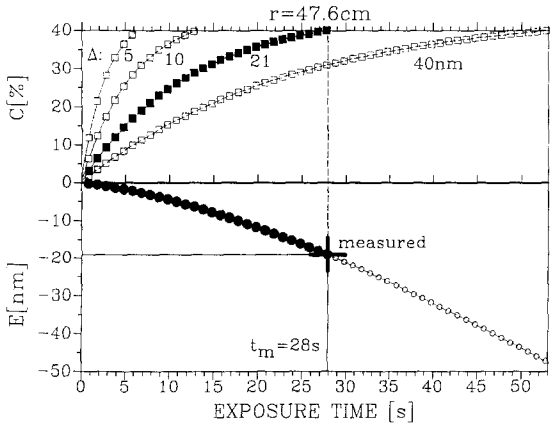

Fig. 5. Example how the fit conditions $c(t) = 40\%$ and $E \approx -20$ nm are satisfied for the observed intermediate time $t_m = 28$ s at $r = 47.6$ cm by variation of the involved thickness ($\Delta = 21$ nm; $f^C = 0.61$, $f^B = 2.15$).

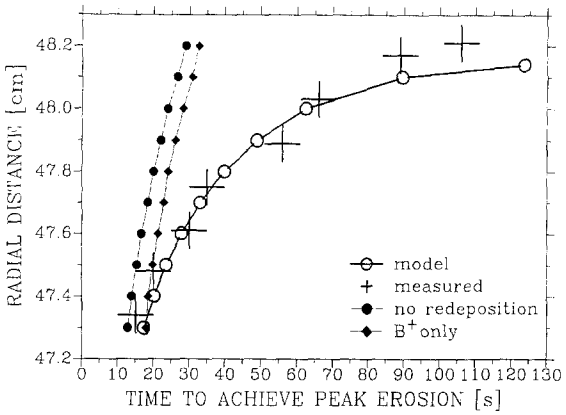

Fig. 6. Measured (crosses) erosion times t_m before peak erosion is achieved depending on radial distance and comparison (circles) with calculations which include a boron redeposition proportional to r. Redeposition by B^+ only (diamonds) or even no redeposition (full circles) do not fit the data.

5. Results

Fig. 6 summarizes the results of the fitting procedure. It shows the times $t_m(r)$ where intermediate erosion turns to peak erosion as measured (crosses) and as calculated (circles), both depending on radial distance r. As before we assumed $Y = 0.0135$. The possible agreement is striking especially in comparison to the other two cases where either the additive term Γ_B^n is neglected (diamonds) or even the boron redeposition at all (dots). The intermediate rates calculated according to Eq. (8) are time averages, but agree as before in the considered range (circles in Fig. 3). If Y is set to the value 0.047 at time t_m the calculated rates jump to the observed peak values of ≈ -6 nm/s. The calculations show that the carbon concentration $c(t)$

can continuously increase within the time t_m up to a value where it triggers the transition from low to high sputter yield, i.e. from slow to fast erosion. The time behavior can be described correctly if boron redeposition is assumed.

6. Conclusions

The model presented can only be a preliminary step to understand the complex processes in layers affected by simultaneous erosion and deposition, and we do not stress the absolute numbers in the equations. Nevertheless, it supports the basic idea that the time evolution $c(t)$ of the carbon concentration in the near surface layer of the boron film rules the erosion speed. The sputter yield Y increases drastically if $c(t)$ exceeds $\approx 40\%$. AES depth profiling shows that the erosion process ends with a carbon rich layer on top of the a-B:D remnants.

The model suggests that the direct redeposition of boron must not be neglected. It decays with time because of the gradual erosion of the boron coating, but decelerates the evolution of $c(t)$. This prolongs the time t_m for the intermediate erosion and hence the life time of the protecting coating in the erosion dominated area. The changing ratio of concentration $b(t)/c(t)$ may also influence the ratio of the BII/CII emission light observed by spectroscopy which usually is understood as being caused by the flux ratio only.

The layer involved seems to have a thickness of ≈ 20 nm which is more than ion stopping power (few nm) of the impurity ions transported in the SOL and hitting the surface. This is not understood yet, but obviously a reason why boron can be eroded in zones of net carbon deposition and why an Al containing C/B deposit remains in the erosion zone even if Al is sputtered out of the substrate.

Colorimetry can measure time resolved, in-situ and on extended areas erosion and deposition rates of protecting coatings in TEXTOR-94 and provides a good data base for modeling. The validation of the quantitative description in terms of a balance of the impurity deposition fluxes in the SOL, of the redeposition fluxes and of the hydrogen erosion with the sputter yield Y as the key parameter becomes possible if additional information from other techniques is used.

References

[1] M.F.A. Harrison, E.S. Hotston and G.P. Maddison, NET Report EUR-FU/80/90-97 (1990).
[2] J. Winter, H.G. Esser, L. Könen et al., J. Nucl. Mater. 162–164 (1989) 713.
[3] P. Wienhold, F. Waelbroeck, H. Bergsåker et al., J. Nucl. Mater. 162–164 (1989) 369.
[4] P. Wienhold and F. Weschenfelder, Vacuum 47(6–8) (1996) 919.
[5] H.G. Esser, J. Winter, V. Philipps et al., J. Nucl. Mater. 220–222 (1995) 457.
[6] P. Wienhold, F. Weschenfelder and J. Winter, Nucl. Instrum. Methods. Phys. Res. B 94 (1994) 503.
[7] A. Pospieszczyk, in: eds. R.K. Janev and H.W. Drawin, Plasma Physics in Controlled Thermonuclear Fusion (1993) p. 213.
[8] K.L. Bell, H.B. Gilbody, J.G. Hughes et al., CLM-R216, UKAEA report (1982).
[9] G.M. McCracken, D.H.J. Goodall, P.C. Stangeby et al., J. Nucl. Mater. 162–164 (1989) 356.
[10] A. Pospieszczyk, V. Philipps, E. Casarotto et al., 22nd Europ. Conf. on Contr. Fus. and Plasma Physics, Bournemouth, UK, 3–7 July 1995.
[11] E. Vietzke, V. Philipps, K. Flaskamp et al., 10th Int. Symp. on Plasma Chem., Bochum, Germany, 4–9 Aug. 1991.
[12] V.M. Sharapov, A.I. Kanaev, S.Yu. Rybakov et al., J. Nucl. Mater. 220–222 (1995) 930.
[13] S. Vepřek, S. Rambert, M. Heintze et al., J. Nucl. Mater. 162–164 (1989) 724.
[14] A. Annen, A. von Keudell and W. Jacob, J. Nucl. Mater. (1996) letter, in print.
[15] D. Naujoks and R. Behrisch, J. Nucl. Mater. 220–222 (1995) 227.
[16] V. Philipps, A. Pospieszczyk, H.G. Esser et al., these Proceedings, p. 105.
[17] U. Kögler, F. Weschenfelder, J. Winter et al., these Proceedings, p. 816.